

A perturbation model of radiometric manifestations of oceanic currents

Oleg A. Godin

Cooperative Institute for Research in Environmental Studies, University of Colorado, NOAA Environmental Technology Laboratory, Boulder, Colorado, USA

Vladimir G. Irisov

Zel Technologies LLC, NOAA Environmental Technology Laboratory, Boulder, Colorado, USA

Received 5 March 2002; revised 21 June 2002; accepted 5 August 2002; published 13 June 2003.

[1] Extracting quantitative oceanographic information from microwave images of the ocean surface requires a physical understanding and an efficient mathematical model of surface wave interaction with currents. In this paper, we consider “weak” currents (with velocities up to a few tens of centimeters per second) and discuss a perturbation approach that leads to numerically efficient models of surface roughness modulation by the current fields with arbitrary dependence on horizontal coordinates and time. With the wave-atmosphere interaction being described within the relaxation approximation, closed-form analytic expressions are obtained for surface roughness modulation. The hydrodynamic theory is combined with an electromagnetic model based on the small-slope approximation to simulate microwave emission from the ocean surface. Analysis of the theoretical results demonstrates that the physics of surface wave interaction with time-dependent currents, which are inhomogeneous in two spatial dimensions, is more rich and complex than is suggested by the one-dimensional models considered theoretically in the past. Of particular interest for remote sensing is the finding that realistic two-dimensionally inhomogeneous currents, unlike their one-dimensional models, can produce perturbations in microwave brightness temperature that extend well beyond the current field itself. Our model suggests that microwave brightness temperature measurements should be a sensitive tool of observing and quantitatively evaluating surface currents in the ocean. *INDEX TERMS:* 0659

Electromagnetics: Random media and rough surfaces; 4275 Oceanography: General: Remote sensing and electromagnetic processes (0689); 4512 Oceanography: Physical: Currents; 4560 Oceanography: Physical: Surface waves and tides (1255); 6959 Radio Science: Radio oceanography; *KEYWORDS:* wave-current interaction, microwave remote sensing, surface roughness modulation, thermal radiation, small-slope approximation, surface wave spectrum

Citation: Godin, O. A., and V. G. Irisov, A perturbation model of radiometric manifestations of oceanic currents, *Radio Sci.*, 38(4), 8070, doi:10.1029/2002RS002642, 2003.

1. Introduction

[2] Synthetic aperture radar (SAR) images of the ocean surface often reveal various bathymetric and oceanographic features, including fronts and internal wave solitons [see, e.g., *Alpers and Hennings*, 1984; *Gasparovic et al.*, 1988; *Hogan et al.*, 1996; *Marmorino et al.*, 1997]. The visibility of underwater physical

processes in radar images is made possible by modulation of the ocean surface-wave spectrum by surface currents associated with the oceanographic and bathymetric features. The surface roughness modulation should also make the oceanographic features visible in microwave brightness temperature maps of the ocean surface. *Kropfli et al.* [1999] demonstrated a remarkable agreement between radar and radiometric observations and in situ measurements of internal wave solitons off the coast of Oregon. These observations suggest a possibility of remote sensing of surface currents in the

This paper is not subject to U.S. copyright.

Published in 2003 by the American Geophysical Union.

ocean with passive radiometric observations in the microwave band.

[3] Extracting quantitative information about oceanographic features from radiometric images of the ocean surface requires a physical understanding and a mathematical model of surface roughness variations due to surface currents, and microwave radiation by a rough surface. The electromagnetic part of the problem is currently well understood and efficient numerical models are available to predict the microwave radiation [Irisov, 1997, 2000]. The fluid-mechanical problem of surface wave interaction with currents has a long history, see reviews by *Peregrine* [1976] and *Peregrine and Jonsson* [1983]. Significant insights have been obtained by theoretical analysis of waves on currents with velocity depending on only one coordinate [Longuet-Higgins and Stewart, 1960, 1961; McKee, 1974; Basovich and Talanov, 1977; Hughes, 1978; Basovich et al., 1987; Thompson et al., 1988; Gotwols et al., 1988; Trulsen et al., 1990; Maltseva et al., 1995; van der Kooij et al., 1995]. Direct numerical integration of equations governing wave train trajectories and wave action balance has been used when simulating surface wave interaction with currents variable in two dimensions [Irvine and Tilley, 1988; Liu et al., 1989; Brissette et al., 1993; Wang et al., 1994].

[4] Calculation of surface-wave spectrum modulation in the broad range of wave numbers required for microwave scattering calculations and for realistic current velocity fields is a computationally intensive problem. In this paper, we present a practical model of surface brightness temperature anomaly due to an arbitrary, horizontally inhomogeneous, and time-dependent current field. We will demonstrate that one-dimensional models fail to capture the essential physics of surface wave modulation by a horizontally inhomogeneous, nonstationary current. Current velocity in the ocean is usually small compared to the group velocity of meter-long and longer surface waves. Using this small parameter, closed-form analytic expressions will be obtained for amplitude and wave vector perturbations of a surface wave due to an inhomogeneous current, leading to a computationally efficient model of surface roughness modulation.

[5] The remainder of the paper is organized as follows. In section 2, the ray theory of surface gravity waves is reviewed, and explicit solutions for wave amplitude and phase modulation by surface currents are obtained assuming that current velocity is small compared to group velocity of the waves. An electromagnetic model of rough surface thermal radiation is presented in section 3. The theory is applied in section 4 to simulate brightness temperature signatures of a seamount in a tidal current. Section 5 summarizes our findings and gives conclusions.

2. Hydrodynamic Model

2.1. Ray Description of Surface Gravity Waves

[6] Assuming temporal and spatial scales of currents to be large compared to period and length of waves, propagation of surface gravity waves can be modeled within the ray approximation [e.g., *Peregrine*, 1976; *Voronovich*, 1976]. Wave trains propagate along rays that obey the following differential equations:

$$\frac{d\mathbf{r}}{d\tau} = \mathbf{c}_g, \quad \mathbf{c}_g = \mathbf{u} + \frac{1}{2} \sqrt{\frac{g}{k}} \frac{\mathbf{k}}{k}, \quad \frac{d\mathbf{k}}{d\tau} = -k_j \nabla u_j, \quad \frac{d\omega}{d\tau} = k \frac{\partial \omega}{\partial t} \quad (1)$$

These equations can be obtained as equations of motion corresponding to the Hamiltonian $H(\mathbf{r}, t; \mathbf{k}, \omega) = (gk)^{1/2} + \mathbf{k} \cdot \mathbf{u} - \omega$. Note that $H = 0$ is equivalent to the dispersion equation $\omega = (gk)^{1/2} + \mathbf{k} \cdot \mathbf{u}$ of linear gravity waves; we disregard effects of nonlinearity on wave dispersion. Here and below, summation over repeated indices $j = 1, 2$ is assumed; g is acceleration due to gravity, t is time, $\mathbf{r} = (x, y)$ is a 2-D position vector on a horizontal plane, \mathbf{c}_g is group velocity in a fixed reference frame (group velocity with respect to the water equals $\mathbf{c}_g - \mathbf{u} = 1/2 g^{1/2} k^{-3/2} \mathbf{k}$), \mathbf{k} and ω are wave vector and frequency, which are related to wave phase θ by $\mathbf{k} = \Lambda \theta$ and $\omega = -M\theta/Mt$. For variation of the phase along the ray we have from equation (1) $d\theta/d\tau = \mathbf{k} \cdot \mathbf{u} - 1/2 (gk)^{1/2}$. The rays described by equation (1) are space-time rays (STRs); these are curves in 3-D space (x, y, t) . Projection of the STR on the horizontal plane (x, y) , according to equation (1), is the trajectory of a particle moving with the group velocity \mathbf{c}_g of the surface wave. The parameter τ specifies the position of a point on the ray.

[7] Variations of wave amplitude along the STR are governed by the wave action balance equation [Keller and Wright, 1975; Hughes, 1978]

$$\partial N / \partial t + \nabla \cdot (\mathbf{c}_g N) = F(N, \mathbf{k}, \mathbf{r}, t), \quad (2)$$

where wave action density N is related to amplitude a of ocean surface elevation in the wave by $N = (\omega - \mathbf{k} \cdot \mathbf{u})^{-1} a^2$. The growth/decay term F in equation (2) describes wave interaction with wind as well as wave dissipation and nonlinear wave interactions. When these processes can be neglected, $F = 0$ and the transport equation (2) expresses wave action conservation. At $F = 0$, the solution to equation (2) is well known in terms of the Jacobian D of the transformation of the Cartesian coordinates to ray coordinates:

$$N(\tau) = \frac{D(\tau_0)}{D(\tau)} N(\tau_0), \quad D(\tau) = \frac{\partial(x, y, t)}{\partial(\alpha, \beta, \tau)}. \quad (3)$$

Ray coordinates are a set of parameters (α, β) that uniquely determine a ray, and a parameter (τ) in equation (3) that specifies a point on the ray. Equation (3) holds regardless of the specific choice of ray coordinates or a reference point $\tau = \tau_0$ on the ray. Calculation of wave amplitude when wave action is not conserved (i.e., $F \neq 0$) will be discussed in section 2.3.

2.2. Waves Riding Upon Weak Currents

[8] When the velocity of currents is small compared to the group velocity of surface waves, the Mach number $M = 2\|u(k/g)^{1/2}\| \ll 1$, and it is convenient to develop unknown $\mathbf{r}(\tau)$, $\mathbf{k}(\tau)$, and $\omega(\tau)$ into powers of the dimensionless small parameter M :

$$\begin{aligned} \mathbf{r} &= \mathbf{r}^{(0)} + \mathbf{r}^{(1)} + \mathbf{r}^{(2)} + \dots, \quad \mathbf{k} = \mathbf{k}^{(0)} + \mathbf{k}^{(1)} + \mathbf{k}^{(2)} \\ &+ \dots, \quad \omega = \omega^{(0)} + \omega^{(1)} + \omega^{(2)} + \dots, \end{aligned} \quad (4)$$

where $|\mathbf{r}^{(s)}| \sim M^s$, $|\mathbf{k}^{(s)}| \sim M^s$, and $|\omega^{(s)}| \sim M^s$, $s = 0, 1, 2, \dots$. Substituting equation (4) into the ray equations (1) and equating coefficients in front of like powers of M , in the zero approximation one obtains

$$\begin{aligned} \mathbf{r}^{(0)}(\tau) &= \mathbf{r}_0 + \frac{1}{2} \sqrt{\frac{g}{k_0}} \frac{k_0}{k_0} \tau, \quad t^{(0)}(\tau) = t_0 + \tau, \quad k^{(0)}(\tau) = k_0, \\ \omega^{(0)}(\tau) &= \omega_0 = \sqrt{gk_0}, \end{aligned} \quad (5)$$

where \mathbf{r}_0 , t_0 , \mathbf{k}_0 , and ω_0 are constants. Obviously, these are equations of STR in the absence of currents. STR is a straight line in the zero approximation. Assuming that a wave train is incident on a current field from infinity, \mathbf{k}_0 and ω_0 have a meaning of the wave vector and frequency of the incident wave.

$$\begin{aligned} \mathbf{r}^{(1)}(\tau) &= \mathbf{r}_0^{(1)} + \int_{-\infty}^{\tau} \mathbf{u}(\mathbf{r}^{(0)}(\tau'), t^{(0)}(\tau')) d\tau' \\ &- \frac{1}{2k_0} \sqrt{\frac{g}{k_0}} \int_{-\infty}^{\tau} d\tau' (\tau - \tau') \\ &\times \left[\mathbf{k}_{0j} \cdot \nabla u_j(\mathbf{r}^{(0)}(\tau'), t^{(0)}(\tau')) - \frac{3\mathbf{k}_0 k_{0j}}{2k_0^2} (\mathbf{k}_0 \cdot \nabla) u_j \right. \\ &\left. \cdot (\mathbf{r}^{(0)}(\tau'), t^{(0)}(\tau')) \right], \end{aligned} \quad (6)$$

[9] In the first approximation, we have from equations (1) and (5): where $\mathbf{r}_0^{(1)}$ is a constant $O(M)$. Here and below, for brevity, we adhere to the following convention: $(M/Mx_j)f(\mathbf{r}^{(0)}, t^{(0)})$, $(M/Mt)f(\mathbf{r}^{(0)}, t^{(0)})$, and the like stand for derivatives $(M/Mx_j)f(\mathbf{r}, t)$, $(M/Mt)f(\mathbf{r}, t)$ evaluated at $\mathbf{r} = \mathbf{r}^{(0)}$, $t = t^{(0)}$, rather than derivatives of

the composite function $f(\mathbf{r}^{(0)}(\mathbf{r}, t), t^{(0)}(\mathbf{r}, t))$. For first-order perturbation to wave vector and frequency we find

$$\begin{aligned} \mathbf{k}^{(1)} &= \nabla \theta^{(1)}, \quad \omega^{(1)} = -\frac{\partial \theta^{(1)}}{\partial t}, \quad \theta^{(1)}(\mathbf{r}, t) = -2k_0 \sqrt{\frac{k_0}{g}} \\ &\cdot \int_0^{+\infty} \mathbf{u} \cdot \left(\mathbf{r} - s \frac{\mathbf{k}_0}{k_0}, t - 2\sqrt{\frac{k_0}{g}} s \right) ds, \end{aligned} \quad (7)$$

where $\theta^{(1)}$ stands for a first-order perturbation in the phase of the wave. According to equation (7), to find wave vector perturbation at a given point and at time t , one has to integrate the gradient of the flow velocity component evaluated at a retarded time, that is, at the moment when the unperturbed ray arrives at the point (x, y) .

[10] In calculating wave amplitude with equation (3), it is convenient to choose the ray coordinates α and β in equation (3) as t_0 (see equation (5)) and y_0 , where y_0 is a limit of $y(\tau)$ at $\tau \rightarrow -\infty$, and hence specifies the position of the incident ray on a wave front. To simplify designations, we choose the Ox coordinate axis along \mathbf{k}_0 . We further designate N_0 the wave action density in the incident wave and choose reference point $\tau = \tau_0$ on the ray at $\tau \rightarrow -\infty$, that is, before the wave train encountered a region with inhomogeneous currents. After some algebra we obtain from equations (3)–(7):

$$\begin{aligned} \frac{N(x, y, t)}{N_0} &= \left[1 + 2\sqrt{\frac{k_0}{g}} u_1(x, y, t) + 2\sqrt{\frac{k_0}{g}} \int_{-\infty}^x dx' \right. \\ &\cdot \left(\frac{\partial u_2}{\partial y} + \frac{1}{2} \frac{\partial u_1}{\partial x} - 2\sqrt{\frac{k_0}{g}} \frac{\partial^2 u_1}{\partial t} \right) - 2\sqrt{\frac{k_0}{g}} \int_{-\infty}^x dx' (x - x') \\ &\cdot \left. \left(\frac{\partial^2 u_1}{\partial y^2} + \sqrt{\frac{k_0}{g}} \frac{\partial^2 u_1}{\partial x \partial t} \right) \right]^{-1} + O(M^2). \end{aligned} \quad (8)$$

As in equation (7), integration in equation (8) is along the unperturbed ray, with derivatives of the flow velocity under the integral being evaluated at the retarded time. Details of derivations that we omitted here are discussed in some detail by Godin [2002] in connection with a related problem of acoustic wave refraction in a weakly inhomogeneous medium. It should be emphasized that, for slowly varying currents, amplitude perturbations rapidly accumulate with the length L of the path within the region of inhomogeneous currents and increase as L^2 ; phase perturbations accumulate more slowly and are proportional to L .

[11] The perturbation results (7) and (8) have been verified against a problem that allows an independent

exact solution, namely, the case of a “one-dimensional” current with the velocity field $\mathbf{u}(\mathbf{r}, t) = \mu u(\mu \cong \mathbf{r} - V t)$, which varies only in one direction. Here μ is a constant unit vector. In particular, the perturbation results agree with the solution obtained by *Longuet-Higgins and Stewart* [1961] for a stationary one-dimensional current ($V = 0$).

[12] For any one-dimensional current that depends on coordinates and time via the combination $\mu \cong \mathbf{r} - V t$, integrals in equations (7) and (8) can be easily solved in terms of the current velocity and its derivatives at \mathbf{r}, t . In general, unlike the one-dimensional case, perturbations in wave vector and amplitude of the wave at a given point depend not only on the local value of the flow velocity at this point, but also on spatial and temporal derivatives of the velocity along the wave train trajectory. In an important special case of potential flow $\mathbf{u} = \mathbf{\Lambda}\varphi(\mathbf{r}, t)$ equations (7) and (8) give

$$\mathbf{k}^{(1)}(x, y, t) = -2k_0 \sqrt{\frac{k_0}{g}} \mathbf{u} + 4 \frac{k_0^2}{g} \int_{-\infty}^x \frac{\partial \mathbf{u}}{\partial t} \cdot \left(x', y, t - 2 \sqrt{\frac{k_0}{g}} (x - x') \right) dx' \quad (9)$$

and

$$\begin{aligned} \frac{N(x, y, t)}{N_0} = & \left[1 + 3 \sqrt{\frac{k_0}{g}} u_1(x, y, z) - 8 \frac{k_0}{g} \int_{-\infty}^x dx' \frac{\partial u_1}{\partial t} \right. \\ & \left. + 4 \frac{k_0}{g} \int_{-\infty}^x dx' (x - x') \cdot \left(\sqrt{\frac{k_0}{g}} \frac{\partial^2 u_1}{\partial t^2} + \frac{\partial^2 u_2}{\partial y \partial t} \right) \right]^{-1} \\ & + O(M^2). \end{aligned} \quad (10)$$

We see that for a potential current, accumulation of wave vector and amplitude perturbations along the wave trajectory is possible only in the nonstationary case. For time-independent currents, the integral terms in the right-hand sides of equations (9) and (10) vanish, and wave vector and wave action variations are due solely to the local current velocity $\mathbf{u}(x, y, t)$. In particular, for a potential stationary current occupying a finite domain on the horizontal plane, there is no perturbation in wave amplitude and wave vector after the wave crosses this domain.

2.3. Wave-Wind Interaction and Other Source Terms

[13] While assumption of wave action conservation appears quite justified for swell, both wave interaction with wind and dissipation become increasingly important

for shorter waves, and a realistic description of meter-long and shorter waves, with or without current, is not possible without an explicit account of the growth-decay term in the wave balance equation (2). Following the work of *Keller and Wright* [1975] and *Hughes* [1978], this term is often modeled in a wave relaxation approximation, with $F < 0$ when wave action density N exceeds certain equilibrium level N_e , which is a function of wind velocity and wave number, and $F > 0$ at $N < N_e$. The relaxation approximation describes the tendency of wave amplitude to return to the equilibrium level sustained by the wind. *Hughes* [1978] assumed $F = \beta N [1 - (N/N_e)^\alpha]$ with $\alpha = 1$ and β being the growth rate of waves, while other authors advocated models with different values of α and β , see a discussion by *Trulsen et al.* [1990]. For the perturbation analysis, specific functional dependence of F on its arguments is not important as long as deviations from the equilibrium are small. Neglecting terms of second and higher order in $N - N_e$, we represent the source term as

$$F = -\gamma(N - N_e), \quad \gamma = -\partial F / \partial N|_{N=N_e} > 0. \quad (11)$$

For the above power law model of the source term $\gamma = (\alpha + 1) \beta$; $1/\gamma$ has the meaning of the relaxation time of perturbed wave amplitude to its equilibrium value.

[14] The wave action balance equation (2) with the source term equation (11) is linear in N and is easily solved analytically. Here we consider only the case where wind velocity is constant and incident waves have equilibrium amplitudes, $N_e = N_0(\mathbf{k})$. Then

$$\begin{aligned} N = N_1(\tau) + N_0(\mathbf{k}(\tau)) \int_{-\infty}^x \gamma \left(1 - \frac{N_1}{N_0} \right) \\ \cdot \exp \left(\int_{\tau}^{\tau_1} \gamma d\tau_2 \right) d\tau_1, \end{aligned} \quad (12)$$

where integration is along a ray that arrives at a given point at a given time; N_1 stands for the solution in the case $\gamma = 0$, which we considered in sections 2.1 and 2.2. As expected, in limiting cases it follows from equation (12) that $N \rightarrow N_0$ at $\tau \rightarrow -\infty$ (the wave has not interacted yet with the current), $N(\tau) \rightarrow N_I(\tau)$ at $\gamma \rightarrow 0$ (negligible wind interaction and wave dissipation), and $N \rightarrow N_e$ at $\gamma \rightarrow +\infty$ (strong interaction). Linearizing equation (12) with respect to current-induced perturbations in ray geometry and amplitude and using equation (10) for the solution N_1 , after some algebra we obtain

$$N(\mathbf{k}; \mathbf{r}, t) = A(\mathbf{k}; \mathbf{r}, t) N_0(\mathbf{k} - \mathbf{B}(\mathbf{k}; \mathbf{r}, t)), \quad (13)$$

where

$$\begin{aligned}
 A(\mathbf{k}, \mathbf{r}, t) &= 1 - 2\sqrt{\frac{k}{g}} \int_0^{+\infty} ds \cdot \exp\left(-\sqrt{\frac{k}{g}}\gamma(\mathbf{k})s\right) \\
 &\quad \cdot \left(\nabla \cdot \mathbf{u} + \frac{k_j}{2k^2} \mathbf{k} \cdot \nabla u_j\right) + \frac{2k_j}{k^2} \int_0^{+\infty} \\
 &\quad \cdot \frac{ds}{\gamma} \left[1 - \exp\left(-\sqrt{\frac{k}{g}}\gamma(\mathbf{k})s\right)\right] \\
 &\quad \cdot \left(k\nabla^2 u_j - \frac{1}{k}(\mathbf{k} \cdot \nabla)^2 u_j + \sqrt{\frac{k}{g}}(\mathbf{k} \cdot \nabla) \frac{\partial u_j}{\partial t}\right), \\
 \mathbf{B}(\mathbf{k}, \mathbf{r}, t) &= -2\sqrt{\frac{k}{g}} k_j \int_0^{+\infty} \exp\left(-\sqrt{\frac{k}{g}}\gamma(\mathbf{k})s\right) \\
 &\quad \cdot \nabla u_j \left(\mathbf{r} - s \frac{\mathbf{k}}{k}, t - 2\sqrt{\frac{k}{g}}s\right) ds. \quad (14)
 \end{aligned}$$

Integrals in equation (14) are taken along unperturbed, straight rays, with derivatives of the current velocity \mathbf{u} being evaluated at the retarded time. Equations (12) and (14) explicitly describe the combined effect of wave refraction by inhomogeneous, time-dependent currents, as well as of varying rate of energy input and loss that changes with wave amplitude and its wave vector. Although obtained with the ray theory, implementation of equations (12)–(14) requires neither ray tracing nor the computationally intensive procedure of finding a ray that comes to a given point at a given time, thus leading to a vastly increased computational efficiency.

2.4. Surface Wave Spectrum Modulation

[15] When ocean surface roughness is considered to be due to a continuum of surface waves with random phases, the spectrum Φ of the elevation ζ is related to the spectrum of wave action density n by $\Phi(\mathbf{k}; \mathbf{r}, t) = n(\mathbf{k}; \mathbf{r}, t)\sigma(\mathbf{k})$, where σ is frequency of the wave in the reference frame following the current; $\sigma = (gk)^{1/2}$ for gravity waves. The wave action spectrum satisfies the equation [Keller and Wright, 1975; Hughes, 1978]

$$\partial n / \partial t + \mathbf{c}_g \cdot \nabla n = F(n, \mathbf{k}, \mathbf{r}, t), \quad (15)$$

which can be solved using a technique that is similar to the one that was applied above to equation (2) for wave action density of an individual wave train. (Solving equation (15) is actually simpler by far than solving equation (2) because no need arises to calculate the Jacobian D of the transformation to ray coordinates.)

For perturbations of the first order in current velocity, the result is given by

$$n(\mathbf{k}; \mathbf{r}, t) = n_0(\mathbf{k} - \mathbf{B}(\mathbf{k}; \mathbf{r}, t)), \quad (16)$$

where \mathbf{B} is defined in equation (14) and $n_0(\mathbf{k})$ stands for the wave action spectrum in the absence of currents. The difference between equations (13) and (16) is due to the fact that focusing or defocusing of wave packets by refraction, which is described by the factor A in equation (13), is exactly compensated for by variation in the spectral band of wave vectors occupied by the wave train [Hughes, 1978; Irvine and Tilley, 1988].

[16] Relaxation time rapidly decreases with wavelength, and for shorter gravity waves, effects due to currents are effectively determined by current velocities in a small vicinity of the observation point. The role of cascade-type nonlinear wave interactions increases when wavelength decreases, and for sufficiently short waves the relaxation model of the source term, which is local in \mathbf{k} and does not describe energy transfer between waves with different \mathbf{k} , ceases to be applicable. Therefore we use the perturbation results derived above only for waves with $k \leq K$. The amplitude of short waves with $k > K$ is determined primarily by energy influx from long waves [Komen *et al.*, 1994, p. 142]. We model this by assuming that modulation of a short-wave spectrum due to currents is independent of wavelength and equals the modulation at separation wave number K : $n(\mathbf{k}; \mathbf{r}, t)/n_0(\mathbf{k}) = n(\mathbf{k}K/k; \mathbf{r}, t)/n_0(\mathbf{k}K/k)$ at $k > K$.

3. Emissivity of the Rough Ocean Surface

[17] We consider a sea surface with a variable “local” roughness spectrum. According to the small slope approximation, the variation of the brightness temperature from its value for a flat water surface can be found as

$$\Delta T_b(\vartheta, \varphi) = T_0 k_0^2 \int \int W(k, \varphi) \cdot R(k/k_0, \vartheta, \varphi - \varphi_1) dk d\varphi_1, \quad (17)$$

where T_0 is the physical temperature of the ocean surface, k_0 is the electromagnetic wave number, $W(k, \varphi)$ is the spectrum of sea waves, which depends also upon location and time, and $R(k, \vartheta, \varphi)$ is a “weighting” function describing a contribution of different wave components to the thermal microwave emission. Expressions for $R(k, \vartheta, \varphi)$ can be found in the work of IrISOV [2000]. Besides a nadir observation angle η , R depends upon a complex dielectric permittivity of seawater and polarization. The spectrum W is defined as a “folded” spectrum $\Phi(\mathbf{k}; \mathbf{r}, t)$: $W(k, \varphi) = [\Phi(k, \varphi) + \Phi(k, \varphi + \pi)]/2$.

[18] In general, brightness temperature contrast ΔT_b dependence on azimuth observation angle φ can be

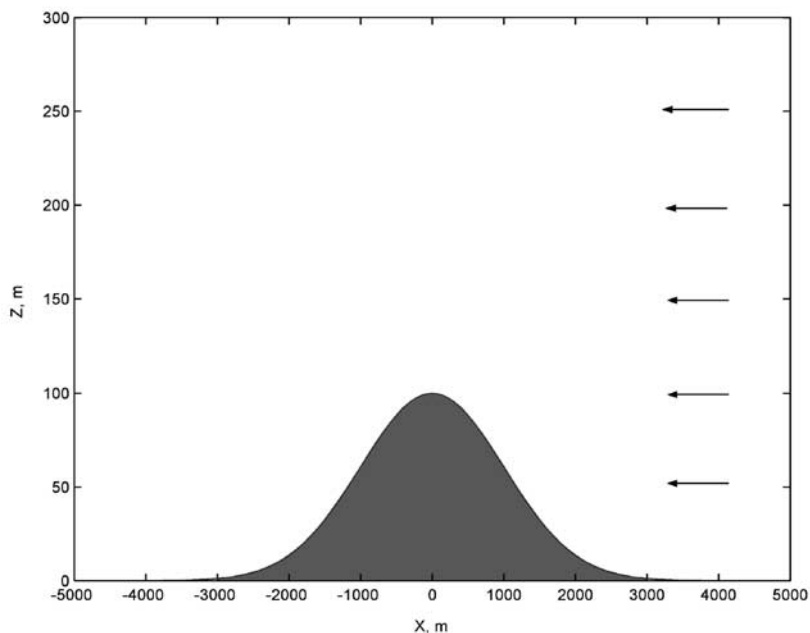


Figure 1. Seamount in the presence of a tidal current of 0.35 m/s from the east. See color version of this figure at back of this issue.

described by the first and second harmonics: $\Delta T_b = A_0 + A_1 \cos \varphi + A_2 \cos 2 \varphi$. Higher-order harmonics are negligible and practically are not observable. Our model, equation (17), describes only 0th and 2nd harmonics, because the modeling of the 1st harmonic requires accounting for non-Gaussian features of the sea surface [see, e.g., *Irisov*, 2000]. It is beyond the scope of this paper. It can be argued that accounting for the 1st harmonic would not result in a noticeable change in the brightness temperature contrast due to inhomogeneous currents.

[19] Expression (17) is a small perturbation approximation for the brightness temperature. Nevertheless, we use it as a small slope approximation utilizing the equivalence between small slope and small perturbation expansions for the brightness temperature of a rough surface [e.g., *Izers et al.*, 1991; *Irisov*, 1997].

[20] In our model we neglect the effect of atmosphere, i.e., downwelling atmospheric radiation scattered from the ocean surface, and attenuation and emission in a layer between a radiometer and the ocean. It is justified for a low-absorption frequency like 37 GHz and low-altitude airborne measurements, when the atmospheric contribution is small. This effect easily can be taken into account, but for the sake of simplicity we neglect it here. Also, we do not consider high wind speed (>12 m/s) when whitecaps and wave breaking become important for micro-

wave thermal radiation. Modeling of such effects should be addressed separately.

4. Numerical Simulation of the Radiometric Signature of a Seamount

[21] For numerical simulation we consider an area 10×10 km² of a 300-m-deep ocean with an axially symmetric seamount. As a function of distance r from the axis, the elevation of the seamount above the ocean floor is described by a Gaussian function $z = h \exp(-r^2/2R^2)$ with $R = 1000$ m and $h = 100$ m (Figure 1). We assume that far from the seamount there is a barotropic tidal current with velocity $V = 0.35$ m/s directed toward the east. Following *Landau and Lifshitz* [1982] and *Miles* [1971], current flow perturbation by the seamount is modeled as a flow due to a dipole source of size R and strength $2\pi R^2 h V$. The 8 m/s wind blows to the east. The background wave spectrum was calculated using the model proposed by *Caudal and Hauser* [1996], which is a spectrum model by *Apel* [1994] with a corrected spreading function. It was assumed that, far from the seamount, the wave spectrum coincided with the background spectrum in a reference frame following the tidal current. The effect of wave growth and dissipation was accounted for using the *Hughes* [1978] relaxation model

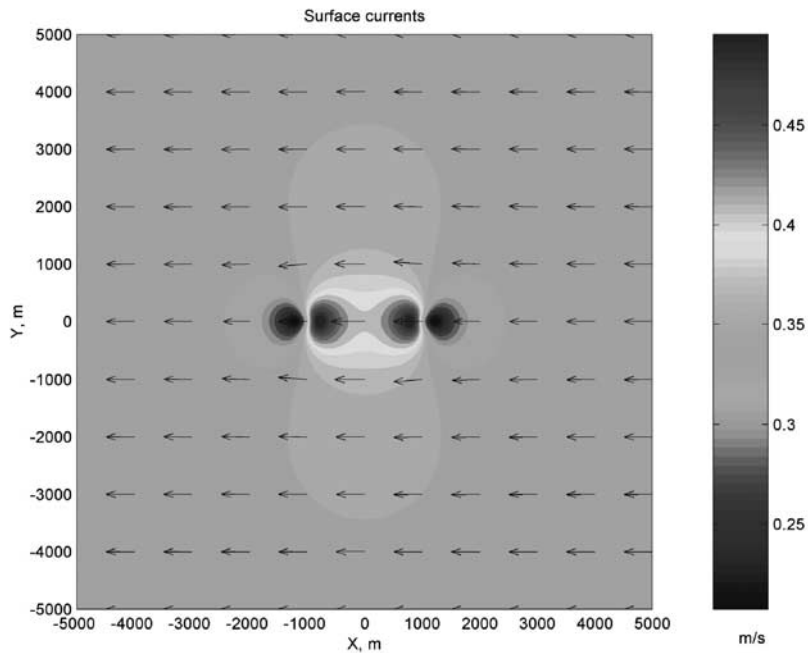


Figure 2. Surface currents disturbed by a seamount. Color designates an absolute value of the surface current. See color version of this figure at back of this issue.

with the growth rate β proposed by *Plant* [1982]. The dielectric permittivity was calculated from the model by *Ellison et al.* [1998]. Sea water temperature was taken as 15°C , salinity as 35‰, and the radiometric frequency as 37 GHz.

[22] These parameters were used to calculate the surface current field (Figure 2), the perturbed wave action, the “local” spectrum of surface elevation, and the brightness temperature at vertical and horizontal polarizations at 54° nadir viewing angle. Azimuthal observation direction was taken toward the north, although the simulations showed that the result is not sensitive to the last parameter.

[23] Numerical integration over wave number k in equation (17) was fulfilled from $k_{min} = 0.5 \text{ m}^{-1}$ to $k_{inf} = 1000 \text{ m}^{-1}$. In calculating the hydrodynamic modulation, $K = 20 \text{ m}^{-1}$ was chosen for the separation wave number. We also estimated brightness temperature variations at $K = 10 \text{ m}^{-1}$ and found that ΔT_b changed by less than 10%. Contribution of the long waves with $k < k_{min}$ to the brightness temperature is negligible.

4.1. Wind Waves on the Ocean Surface

[24] In this section, we consider the “direct” effect of the dipole current on wave spectrum and consequently on microwave brightness temperature. Figure 3 shows

the brightness temperature contrast map, i.e., the difference due to surface roughness, at vertical (a) and horizontal (b) polarizations. The contrast at vertical polarization is noticeably smaller than that at horizontal polarization. This is an expected result related to the specifics of the microwave radiation from the ocean at vertical polarization; the contrast changes the sign somewhere around a 50° – 60° observation angle. Nevertheless, even at vertical polarization we can expect quite a strong signature from a seamount. It is even stronger at horizontal polarization: up to 2.2 K variations near the top of the mountain. Note that the brightness temperature patterns shown in Figure 3 are stable in time and space, and so can be easily averaged coherently to improve the signal-to-noise ratio.

4.2. Wind Waves and Swell on the Ocean Surface

[25] In this section, we study the effect of swell as a “mediator” between the surface current perturbation and waves shorter than 10 m. For modeling purposes we consider a monochromatic 60 m swell with an amplitude of 0.5 m and propagating to the east-northeast (at 20° with respect to tidal current direction). Swell modulation is found according to equations (13)–(14) and then swell currents modulate wind wave spectrum according to equation (16). This “cascade” interaction creates notice-

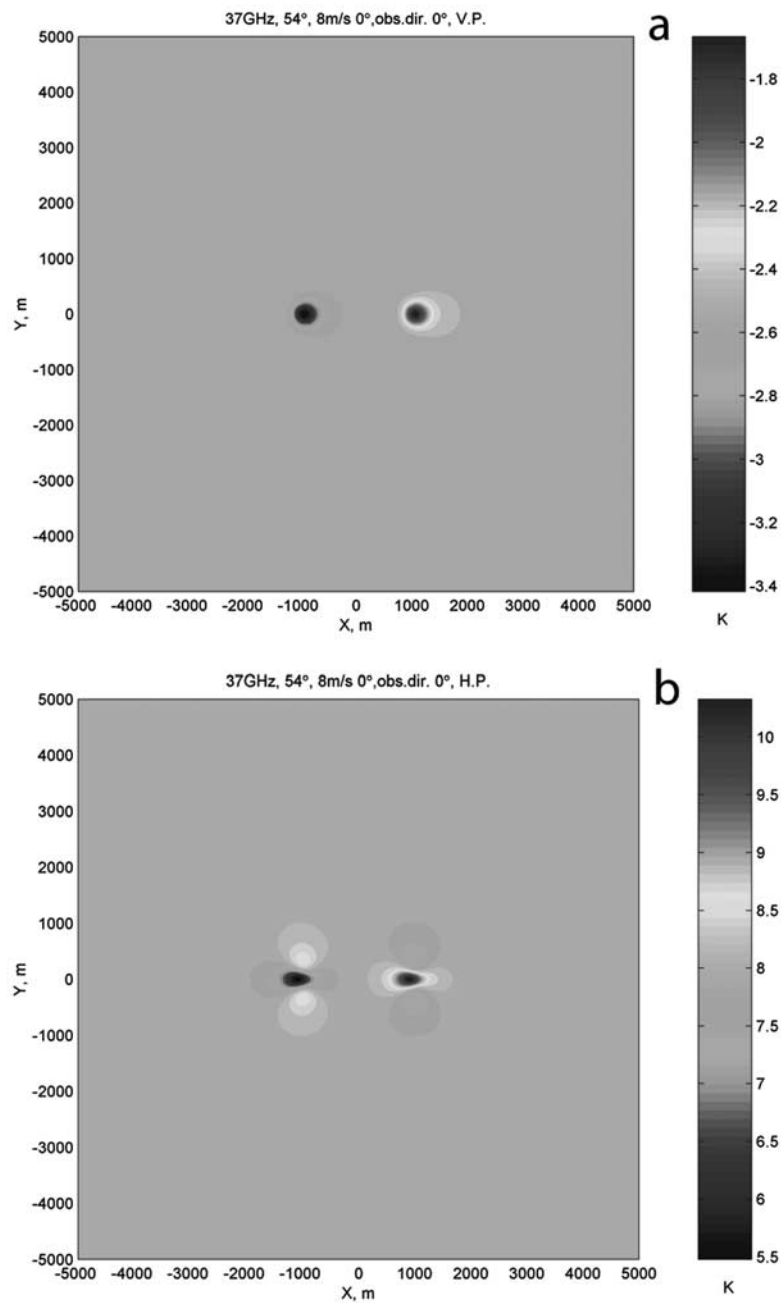


Figure 3. Map of brightness temperature contrast from wave spectrum modulated by dipole surface currents. (a) Vertical polarization. (b) Horizontal polarization. See color version of this figure at back of this issue.

able variations of the brightness temperature despite the fact that the direct effect of swell on the brightness temperature is very weak. Keeping in mind rather high group velocity and weak attenuation of the swell, one can

expect brightness variations extending far beyond the region occupied by an inhomogeneous surface current.

[26] Figure 4 shows the brightness temperature map at vertical (a) and horizontal (b) polarizations. A disturbance

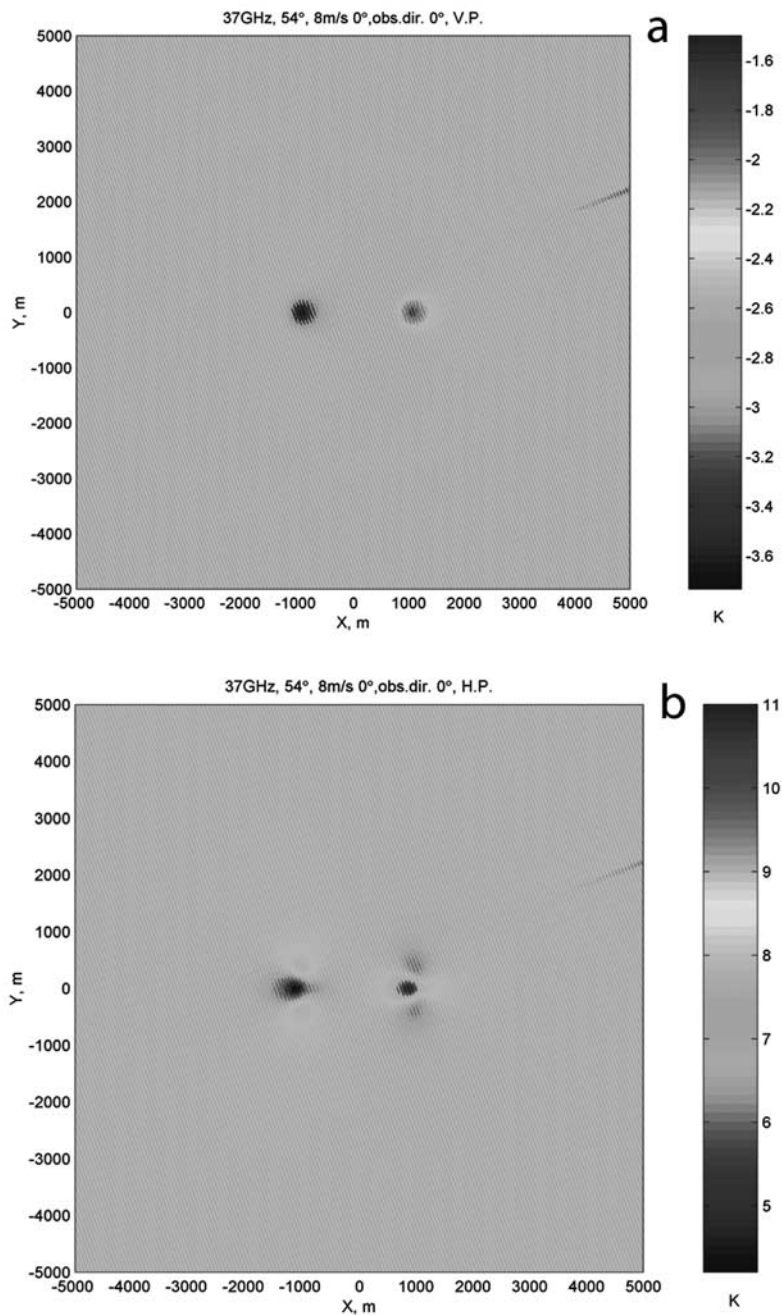


Figure 4. Map of brightness temperature contrast from modulated wave spectrum in the presence of 60 m swell of amplitude 0.5 m. Swell propagates toward the east at 20° with respect to the horizontal axis. (a) Vertical polarization. (b) Horizontal polarization. See color version of this figure at back of this issue.

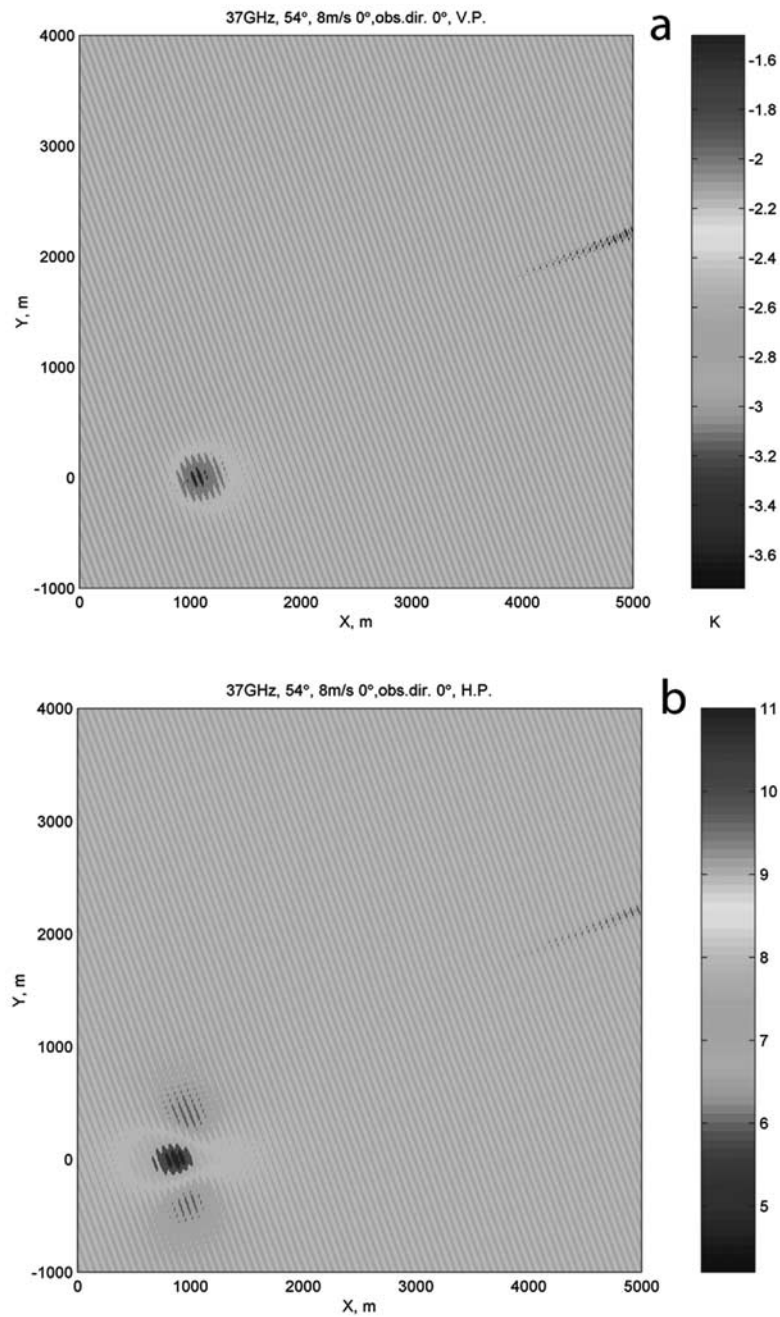


Figure 5. Northeast section of Figure 4 illustrating swell effect on a background wind wave spectrum. (a) Vertical polarization. (b) Horizontal polarization. See color version of this figure at back of this issue.

of the swell field caused by the dipole currents reveals itself as a chain of hot and cold spots a few kilometers away from the seamount. The brightness temperature contrast is rather high and should be easily observable

by a microwave radiometer. An overall “strip” structure of the pattern that can be seen in Figure 5, showing northeast fragments of Figure 4, originates from short waves modulated by the monochromatic swell.

5. Summary and Conclusions

[27] In this paper, we have presented a practical model for simulating brightness temperature variations due to horizontally inhomogeneous, time-dependent currents on the ocean surface. The currents change the brightness temperature by refracting surface waves and thus modulating ocean surface roughness. Computational efficiency of the model is achieved by using the ray theory and analytically solving equations governing surface gravity waves to calculate the surface roughness. Our model predicts that emissivity variations are a sensitive measure of surface currents, with brightness temperature contrasts up to 6 K resulting from currents with velocities less than 25 cm/s in the examples considered. For the purposes of identification of oceanographic processes and bathymetric features in brightness temperature maps, it is important to realize that the relation between temperature variation and current velocity is generally not local. This is because perturbations in surface wave amplitude and wave vector by horizontally inhomogeneous currents, unlike currents inhomogeneous in one dimension, can accumulate along the trajectory of the wave. Another manifestation of the perturbation accumulation along the surface wave trajectory is the appearance of large-scale temperature features that extend well beyond the region of inhomogeneous currents. These features may be helpful in detecting smaller-scale changes in bathymetry, especially with satellite-based radiometers.

[29] **Acknowledgments.** We gratefully acknowledge numerous fruitful and enlightening discussions with Alexander G. Voronovich on the physics of wave-current interaction on the ocean surface. Helpful comments by anonymous reviewers are appreciated.

References

- Alpers, W., and I. Hennings, A theory of the imaging mechanism of underwater bottom topography by real and synthetic aperture radar, *J. Geophys. Res.*, *89*, 10,529–10,546, 1984.
- Apel, J., An improved model of the ocean surface wave vector spectrum and its effects on radar backscatter, *J. Geophys. Res.*, *99*, 16,269–16,291, 1994.
- Basovich, A. Y., and V. I. Talanov, On the transformation of short surface waves on non-uniform currents, *Izv. Russ. Acad. Sci. Atmos. Oceanic Phys.*, *13*, 514–519, 1977.
- Basovich, A. Y., V. V. Bakhanov, and V. I. Talanov, Transformation of wind-driven wave spectra by short internal wave trains, *Izv. Russ. Acad. Sci. Atmos. Oceanic Phys.*, *23*, 520–528, 1987.
- Brissette, F. P., I. K. Tsanis, and J. Wu, Wave directional spectra and wave-current interaction in lake St. Clair, *J. Great Lakes Res.*, *19*, 553–568, 1993.
- Caudal, G., and D. Hauser, Directional spreading function of the sea wave spectrum at short scale, inferred from multi-frequency radar observations, *J. Geophys. Res.*, *101*, 16,601–16,613, 1996.
- Ellison, W., A. Balana, G. Delbos, K. Lamkaouchi, L. Eymard, C. Guillou, and C. Prigent, New permittivity measurements of seawater, *Radio Sci.*, *33*, 639–648, 1998.
- Gasparovic, R. F., J. R. Apel, and E. S. Kasischke, An overview of the SAR Internal Wave Signature Experiment, *J. Geophys. Res.*, *93*, 12,304–12,316, 1988.
- Godin, O. A., A 2-D description of sound propagation in a horizontally-inhomogeneous ocean, *J. Comput. Acoust.*, *10*, 123–151, 2002.
- Gotwols, B. L., R. E. Sterner II, and D. R. Thompson, Measurement and interpretation of surface roughness changes induced by internal waves during the Joint Canada-U.S. Ocean Wave Investigation Project, *J. Geophys. Res.*, *93*, 12,265–12,281, 1988.
- Hogan, G. G., R. D. Chapman, and D. R. Thompson, Observations of ship-generated internal waves in SAR images from Loch Linnhe, Scotland, and comparison with theory and in situ internal wave measurements, *IEEE Trans. Geosci. Remote Sens.*, *34*, 532–542, 1996.
- Hughes, B. A., The effect of internal waves on surface wind waves, 2: Theoretical analysis, *J. Geophys. Res.*, *83*, 455–465, 1978.
- Irisov, V. G., Small-slope expansion for thermal and reflected radiation from a rough surface, *Waves Rand. Media*, *7*, 1–10, 1997.
- Irisov, V. G., Azimuthal variations of the microwave radiation from a slightly non-Gaussian sea surface, *Radio Sci.*, *35*, 65–82, 2000.
- Irvine, D. E., and D. G. Tilley, Ocean wave directional spectra and wave-current interaction in the Agulhas from the shuttle imaging radar-B synthetic aperture radar, *J. Geophys. Res.*, *93*, 15,389–15,401, 1988.
- Izers, A. B., A. A. Puzenko, and I. M. Fuks, The local perturbation method for solving the problem of diffraction from a rough surface with small slope irregularities, *J. Electromagn. Waves Appl.*, *5*, 1419–1435, 1991.
- Keller, W. C., and J. W. Wright, Microwave scattering and the straining of wind-generated waves, *Radio Sci.*, *10*, 139–147, 1975.
- Komen, G. J., L. Cavaleri, M. Donelan, K. Hasselmann, S. Hasselmann, and P. A. E. M. Janssen, *Dynamics and Modelling of Ocean Waves*, Cambridge Univ. Press, New York, 1994.
- Kropfli, R. A., L. A. Ostrovski, T. P. Stanton, E. A. Skirta, A. N. Keane, and V. Irisov, Relationships between strong internal waves in the coastal zone and their radar and radiometric signatures, *J. Geophys. Res.*, *104*, 3133–3148, 1999.
- Landau, L. D., and E. M. Lifshitz, *Course of Theoretical Physics*, vol. 6, *Fluid Mechanics*, Pergamon, New York, 1982.

- Liu, A. K., F. C. Jackson, and E. J. Walsh, A case study of wave-current interaction near an oceanic front, *J. Geophys. Res.*, *94*, 16,189–16,200, 1989.
- Longuet-Higgins, M. S., and R. W. Stewart, Changes in the form of short gravity waves on long waves and tidal currents, *J. Fluid Mech.*, *8*, 565–585, 1960.
- Longuet-Higgins, M. S., and R. W. Stewart, The changes in amplitude of short gravity waves on steady non-uniform currents, *J. Fluid Mech.*, *10*, 529–549, 1961.
- Maltseva, I. G., M. N. Marov, N. S. Ramm, V. R. Fuks, and A. Y. Ivanov, Analysis of kinematic mechanism of ocean internal wave imagery on space SAR images, *Earth Observ. Remote Sens.*, *13*, 409–418, 1995.
- Marmorino, G. O., D. R. Thompson, and C. L. Trump, Correlation of oceanographic signatures appearing in synthetic aperture radar and interferometric synthetic aperture radar imagery with in situ measurements, *J. Geophys. Res.*, *102*, 18,723–18,736, 1997.
- McKee, W. D., Waves on a shearing current: A uniformly valid asymptotic solution, *Proc. Cambridge Philos. Soc.*, *75*, 295–301, 1974.
- Miles, J. W., Internal waves generated by a horizontally moving source, *Geophys. Fluid Dyn.*, *2*, 63–87, 1971.
- Peregrine, D. H., Interaction of water waves and currents, in *Advances in Applied Mechanics*, vol. 16, edited by C. S. Yih, pp. 9–117, Academic, San Diego, Calif., 1976.
- Peregrine, D. H., and I. G. Jonsson, Interaction of waves and currents, *Misc. Rep. 83-6*, Coastal Eng. Res. Cent., U.S. Army Corps of Eng., Fort Belvoir, Va., 1983.
- Plant, W. J., A relationship between wind stress and wind slope, *J. Geophys. Res.*, *87*, 1961–1967, 1982.
- Thompson, D. R., B. L. Gotwols, and R. E. Sterner, II, A comparison of measured surface-wave spectral modulations with predictions from a wave-current interaction model, *J. Geophys. Res.*, *93*, 12,339–12,343, 1988.
- Trulsen, G. N., K. B. Dysthe, and J. Trulsen, Evolution of a gravity wave spectrum through a current gradient, *J. Geophys. Res.*, *95*, 22,141–22,151, 1990.
- Van der Kooij, M. W. A., J. Vogelzang, and C. J. Calkoen, A simple analytical model for brightness modulations caused by submarine sand waves in radar imagery, *J. Geophys. Res.*, *100*, 7069–7082, 1995.
- Voronovich, A. G., Propagation of internal and surface gravity waves in geometrical optics approximation, *Izv. Russ. Acad. Sci. Atmos. Oceanic Phys.*, *12*, 850–857, 1976.
- Wang, D. W., A. K. Liu, C. Y. Peng, and E. A. Meindl, Wave-current interaction near the Gulf Stream during the Surface Wave Dynamics Experiment, *J. Geophys. Res.*, *99*, 5065–5079, 1994.

O. A. Godin, CIRES, University of Colorado and NOAA/Environmental Technology Laboratory, Mail Code R/ET1, 325 Broadway, Boulder, CO 80305-3328, USA. (Oleg.Godin@noaa.gov)

V. G. Irisov, Zel Technologies, LLC and NOAA/Environmental Technology Laboratory, Mail Code R/ET1, 325 Broadway, Boulder, CO 80305-3328, USA. (Vladimir.Irisov@noaa.gov)

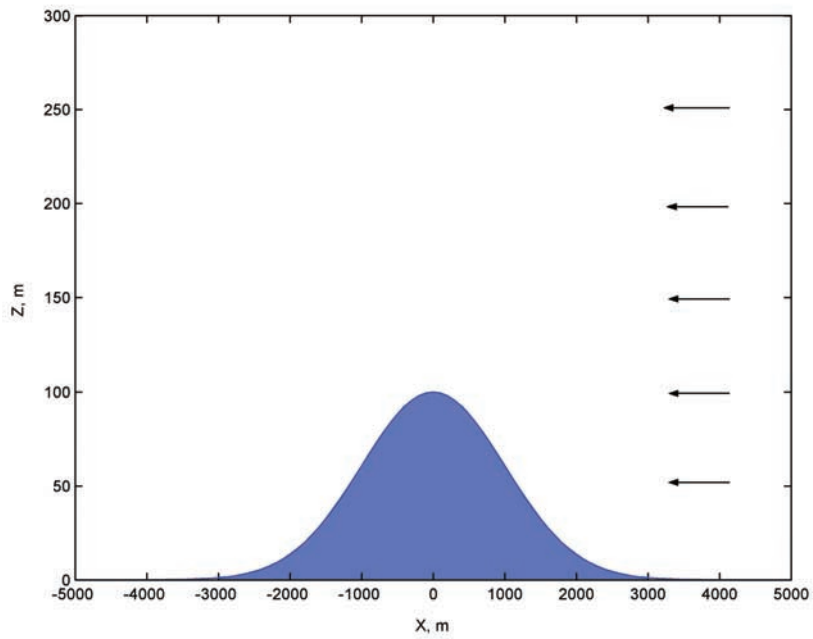


Figure 1. Seamount in the presence of a tidal current of 0.35 m/s from the east.

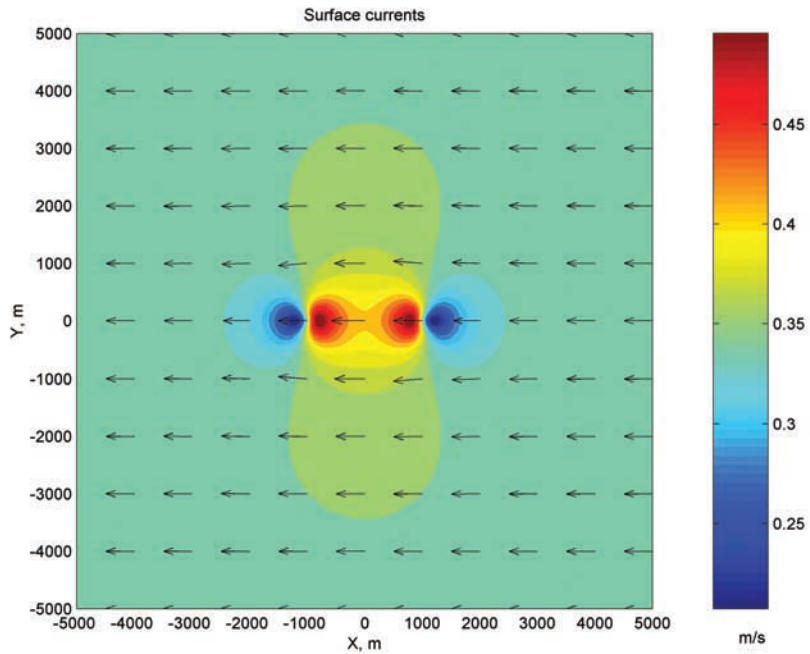


Figure 2. Surface currents disturbed by a seamount. Color designates an absolute value of the surface current.

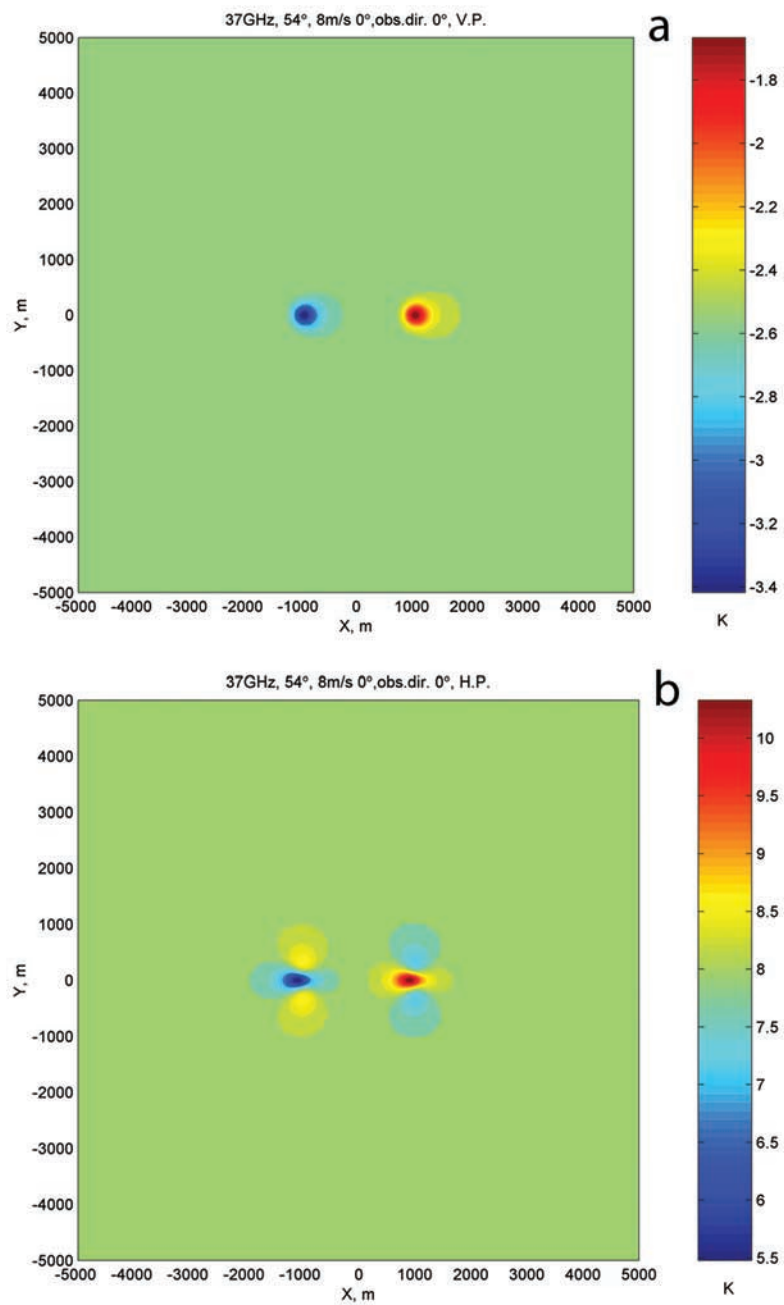


Figure 3. Map of brightness temperature contrast from wave spectrum modulated by dipole surface currents. (a) Vertical polarization. (b) Horizontal polarization.

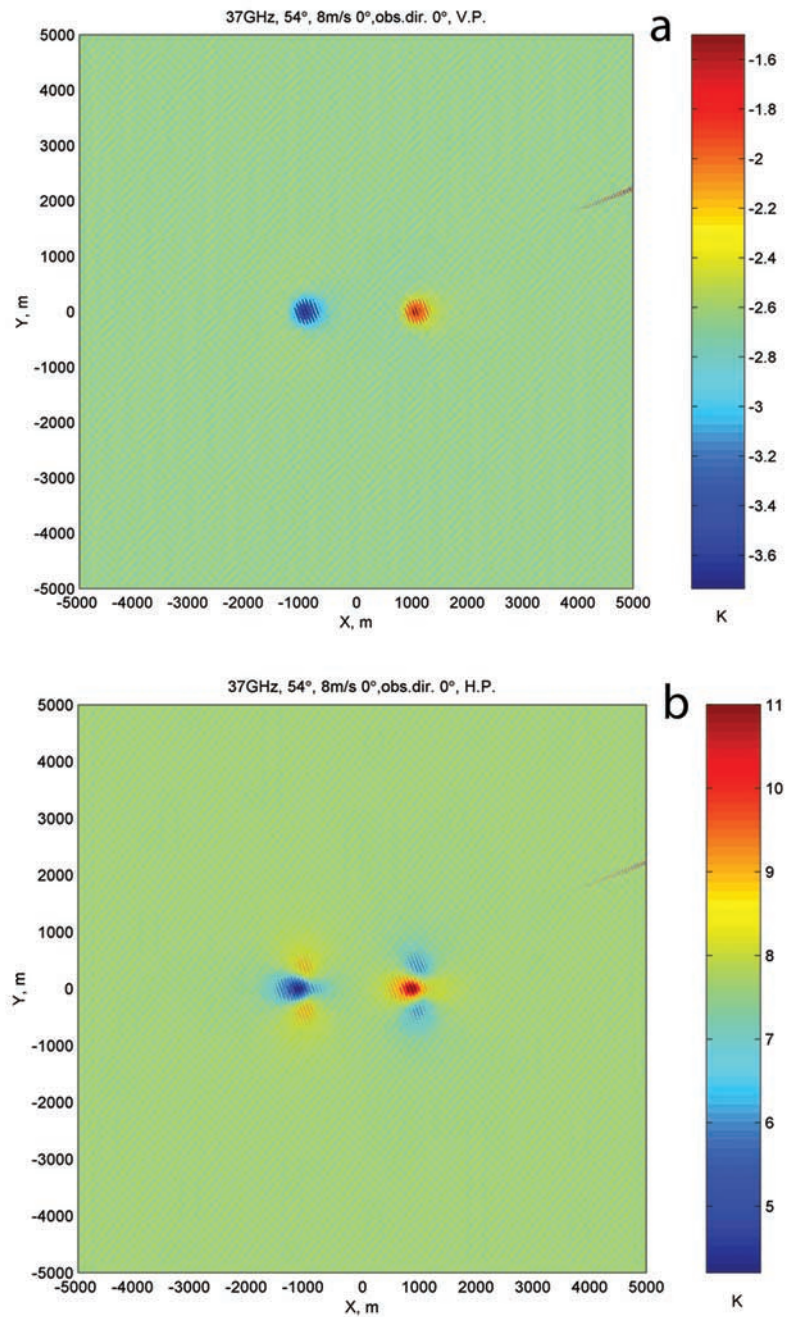


Figure 4. Map of brightness temperature contrast from modulated wave spectrum in the presence of 60 m swell of amplitude 0.5 m. Swell propagates toward the east at 20° with respect to the horizontal axis. (a) Vertical polarization. (b) Horizontal polarization.

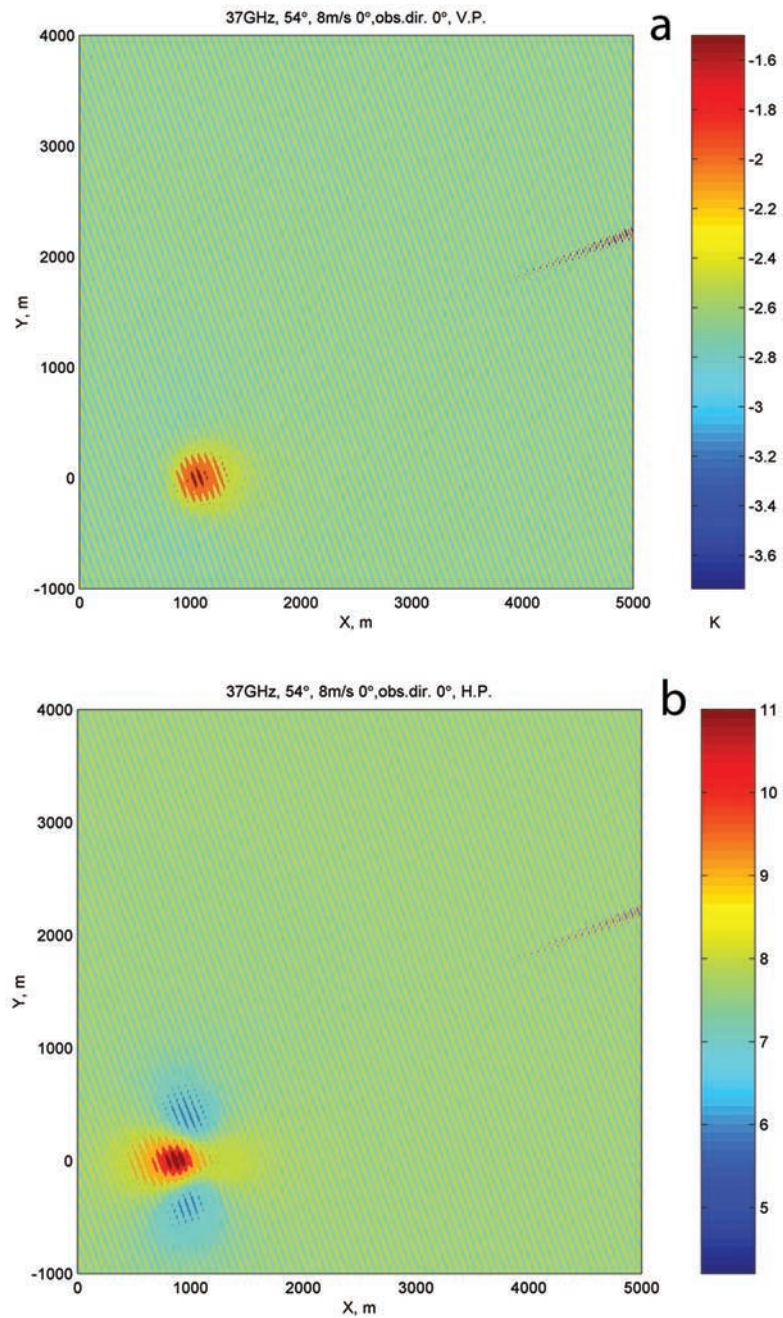


Figure 5. Northeast section of Figure 4 illustrating swell effect on a background wind wave spectrum. (a) Vertical polarization. (b) Horizontal polarization.